Journal of Biomedical Informatics 119 (2021) 103819

Contents lists available at ScienceDirect

Journal of Biomedical Informatics

journal homepage: www.elsevier.com/locate/yjbin

Original Research

An effective feature extraction method based on GDS for atrial fibrillation detection

Haiyan Wang [a,b,c], Honghua Dai [c,d], Yanjie Zhou [e,*], Bing Zhou [c,f], Peng Lu [c,g], Hongpo Zhang [a,c], Zongmin Wang [a,c]

[a] State Key Laboratory of Mathematical Engineering and Advanced Computing, Zhengzhou 450003, China
[b] Simulation Experiment Centre, Zhengzhou University of Aeronautics, Zhengzhou 450046, China
[c] Collaborative Innovation Centre for Internet Healthcare, Zhengzhou University, Zhengzhou 450052, China
[d] Institute of Intelligent Systems, Deakin University, Burwood, VIC 3125, Australia
[e] School of Management Engineering, Zhengzhou University, Zhengzhou 450001, China
[f] School of Information Engineering, Zhengzhou University, Zhengzhou 450001, China
[g] School of Electrical Engineering, Zhengzhou University, Zhengzhou 450001, China

ARTICLE INFO

Keywords:
Atrial fibrillation
Feature extraction
Gradient set
Statistical distribution features
Information quantity features
DNN

ABSTRACT

Atrial fibrillation (AF) is a common and extremely harmful arrhythmia disease. Automatic detection of AF based on ECG helps accurate and timely detection of the condition. However, the existing AF detection methods are mostly based on complex signal transformation or precise waveform localization. This is a big challenge for complex, variable, and susceptible ECG signals. Therefore, we propose a simple feature extraction method based on gradient set (GDS) for AF detection. The method first calculates the GDS of the ECG segment and then calculates the statistical distribution feature and the information quantity feature of the GDS as the input of the classifier. Experiments on four databases include 146 subjects show that the feature extraction method for detecting AF proposed in this paper has the characteristics of simple calculation, noise tolerance, and high adaptability to all kinds of classifiers, and got the best performance on the DNN classifier we designed. Therefore, it is a good choice for feature extraction in AF detection.

1. Introduction

Atrial fibrillation (AF) is a common arrhythmia disease in clinical practice, which can induce angina pectoris, heart failure, and cerebral embolism and has high disability and mortality rates. The timely and accurate detection of AF has important clinical significance, so many researchers are currently working on the automatic detection of AF based on ECG. As shown in Fig. 1, it can be seen that the differences between AF rhythm (below) and normal sinus rhythm (above) in the ECG are [1]: the P-wave disappears; f-waves have widely varying shapes; the R-R interval is not uniform. According to these features, the methods for detecting AF are roughly divided into the following categories: based on R-R interval (RRI) feature, based on P-wave absence (PWA) feature, features based on mathematical transformation, no need to extract features and use deep learning methods directly.

RRI features are most widely used [2-7], *Sadr et al.*[3] extracted 122 features including time domain, frequency domain, and statistical distribution features from RRI and ΔRRI (the change in RRI) as the feature set for AF detection. *Kennedy et al.*[4] used four RRI measurements to train AF detection models: the coefficient of sample entropy (*CoSEn*), the coefficient of variance (*CV*), Root mean square of the successive differences (*RMSSD*), and median absolute deviation (*MAD*). *Andersen et al.*[5] proposed a deep learning model combined with CNN and RNN to extract high-level features from segments of RR intervals to detect AF. *Zhou et al.*[6] proposed a real-time AF detection algorithm based on the heart rate's instantaneous state, which achieved good results; this method adopts the heart rate sequence which can be calculated from the RRI, through a series of conversions and using threshold discrimination to detect AF. *Andersson et al.*[7] detected AF based on three parameters of RRI: turning point ratio, root mean square of successive differences, and Shannon entropy. However, irregular RRI features require a long-term ECG segment to be concluded, which has limitations in processing AF detection of short ECG segments (less than 1 min)[8].

* Corresponding author.
E-mail address: ieyjzhou@zzu.edu.cn (Y. Zhou).

https://doi.org/10.1016/j.jbi.2021.103819
Received 10 January 2021; Received in revised form 29 April 2021; Accepted 16 May 2021
Available online 23 May 2021

PWA features are also widely used, and sometimes they choose to combine RRI features. *Christov et al.*[9] used PWA characteristics combined with detection of atrial arrhythmia to form a combined algorithm to detect AF. *Carlson et al.*[10] also used a change in P-wave morphology when atrial fibrillation occurs to indicate atrial conduction defects. *Ladavich* and *Ghoraani*[11]first created a Gaussian mixture model (GMM) of the P-wave feature space and then used this model to identify PWA and detect AF. *Liu et al.*[12] extracted a total of 33 features, including RRI and PWA-related features to detect AF from a single lead ECG recording. The PWA feature's main problem is that the P wave is not easy to identify, and the P wave is easily masked when the signal is noisy. Both RRI and PWA features require beat detection, so their performance depends on beat detection performance. The ECG signal waveform is complex and variable, which makes beat detection extremely error-prone.

Some researchers use mathematical transformation to extract features, which avoids the R-peak or P-peak detection. For example, *Asgari* and others[13] used the stationary wavelet transform (SWT) to transform ECG signal. Although such methods do not require beat detection, they generally require complex calculations, the accuracy and efficiency may vary greatly when dealing with large data sets [14].

At present, it is more popular to use deep learning algorithms to detect AF, which is an end-to-end model that does not require feature extraction. *Andersen et al.* [5] and *Pourbabaee et al.*[15] directly use the segments of RRIs and raw ECG time-series data as inputs to the deep learning model, respectively. Although the method can achieve good performance, the model interpretability has always been the focus of debate, especially in the medical field.

Aiming at the existing feature extraction methods' challenges, we propose a simple feature extraction method based on the gradient set (GDS) for AF detection. Since the gradient can reflect the change of the waveform at each moment. This method obtains the GDS by the coordinates of all sampling points of the ECG segment, then calculates the statistical distribution features and information quantity feature of the GSD as inputs to the classifier. The proposed feature extraction method does not require heartbeat detection or long-term ECG segment. Although experiments show that the longer the ECG segment, the better the performance, yet the 2 s ECG segment also has good detection results. We also propose a simple deep neural network(DNN), verifying that the proposed method applies to all types of classifiers.

We did multiple experiments on 5 data sets composed of 4 databases, which confirmed the optimal process of this method and proved its effectiveness and superiority. The remainder of this paper is organized as follows. Section 2 introduces the proposed feature extraction method and DNN classifier. Section 3 provides a description of the data used in the experiment, the design and the experiments' results. In section 4, the performance of the feature extraction method proposed in this paper is comprehensively compared with that of other AF detectors. Finally, Section 5 is the conclusion.

2. Methods

2.1. Overview

Fig. 2 shows the general process of automatic AF detection with the morphology-based feature extraction method. The process consists of three main steps:

(1) Preprocessing: The AF and normal rhythm (N) segments of each ECG record are first obtained, and then they are cut into segments of equal length. The length of the equal-length segments is called the window length (WL). The noise reduction step requires comparative experiments and determines the necessity based on the comparison results.
(2) Feature extraction: First get the GDS of the specific WL, such as 2, 5, 8, 10 s. Then calculate the statistical distribution characteristics of the GDS including skewness coefficient (*SKW*), coefficient of variation (*CV*), mode (*MO*), and an information quantity feature information entropy (*ETY*). The normalization step requires a comparison experiment and determines its necessity based on the comparison results.
(3) Classification: The features obtained in step (2) are input into various types of classifiers, and finally, the results are analyzed according to the classification evaluation indicators.

2.2. Preprocessing

The preprocessing phase mainly includes data downsampling, data segmentation, and noise reduction.

To verify the validity of the proposed feature extraction method, it is necessary to test it on different databases. The data come from different databases with different sampling rates. To ensure the accuracy of experimental results, equidistant sampling is adopted for databases to make their sampling rates as consistent or close as possible. The principle is to ensure that the time interval between adjacent sample points for which all data is used to calculate the gradient is consistent.

First, extract the complete AF rhythm segments and N segments of the original ECG record, and then cut them into specific WL segments,

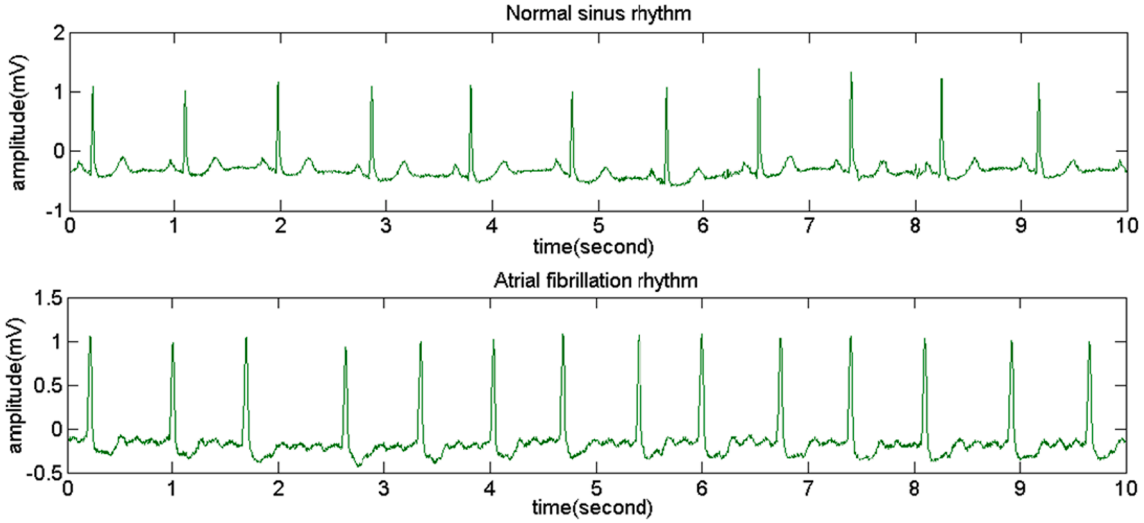

Fig. 1. ECG signals of normal sinus rhythm and AF rhythm.

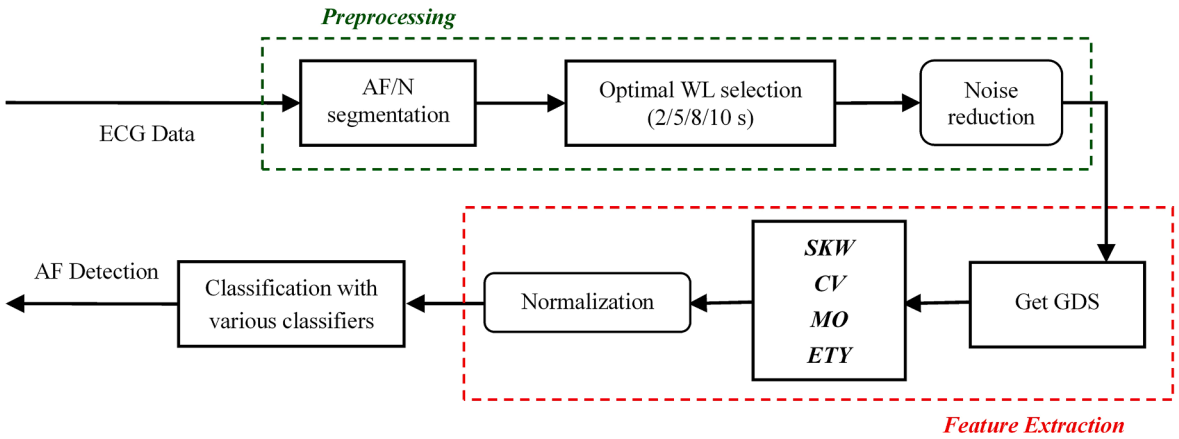

Fig. 2. The framework of the proposed method for AF detection.

the optimal WL needs to be determined experimentally here.

ECG noise mainly comes from myoelectric interference and baseline wander. In this paper, Butterworth and zero phase shift filters are used to remove the myoelectric interference and baseline wander, respectively. The denoising process and effect are shown in Fig. 3. The top is the original ECG signal. The middle is the ECG signal after the myoelectric interference is removed. The bottom is the ECG signal after removing myoelectric interference and baseline wander. Experiments are needed to verify if noise reduction is needed.

2.3. Feature extraction

Fig. 2 shows that feature extraction can be roughly divided into two stages, GDS acquisition, and feature set acquisition, respectively.

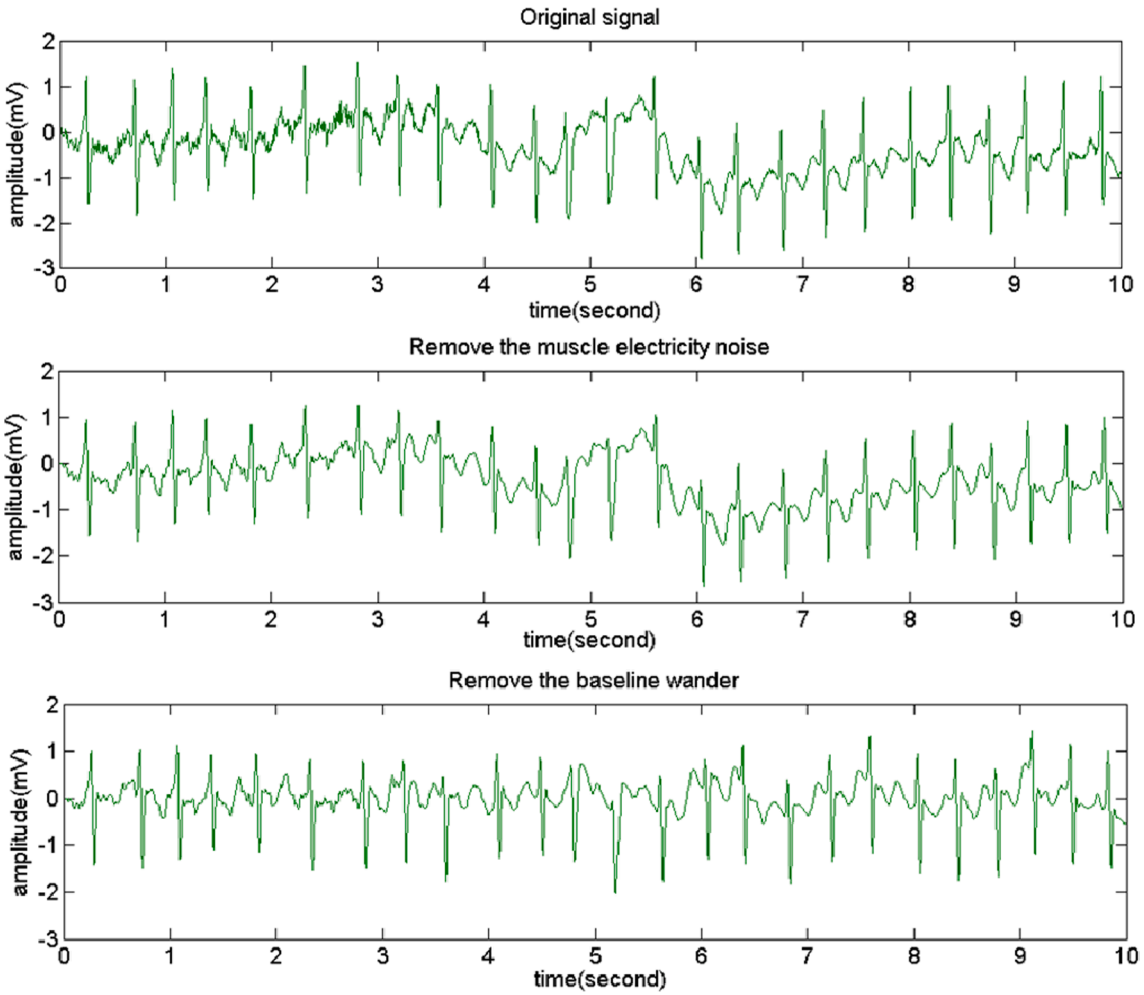

Fig. 3. Example of denoising: original signal (top row); the signal with myoelectric interference removed (middle row); the signal with myoelectric interference and baseline wander removed (bottom row).

2.3.1. GDS acquisition

First, the GDS of each specific WL segment needs to be obtained. The calculation for obtaining the gradient is very simple, as shown in formula (1); n represents the number of sampling points of the specific WL segment, and A_{i+1} and A_i represent the amplitude of the $(i+1)$-th and i-th sampling points, respectively. Δt represents the time interval between the $(i+1)$-th and i-th sampling points, and s_{i+1} represents the gradient of the $(i+1)$-th sample point. The GDS S of each specific WL segment contains $n-1$ gradient values.

$$s_{i+1} = (A_{i+1} - A_i)/\Delta t (i = 1, 2, 3, \cdots, n-1) \tag{1}$$

$$S = \left[s_2, s_3, \cdots, s_{(n-1)+1} \right]$$

2.3.2. Feature set acquisition

To comprehensively acquire the features of each dataset, the statistical distribution features and information quantity feature of the GDS are extracted. *CV*, *SKW*, and *MO* are selected as statistical distribution features, which respectively can reflect the degree of distribution dispersion, the distribution form, and the distribution centralization trend of a dataset. The information quantity feature is represented by *ETY*, which is a quantitative measure of the information contained in the dataset.

1. CV(Coefficient of variation)

The *CV*, also known as 'discrete coefficient', is a normalized measure of the dispersion degree of a probability distribution.

$$CV(S) = S_\sigma / S_\mu \tag{2}$$

$$S_\mu = \frac{1}{n-1}\sum_{i=1}^{n-1} s_i, \quad S_\sigma = \sqrt{\frac{1}{n-1}\sum_{i=1}^{n-1}(s_i - S_\mu)^2}$$

CV is defined as the standard deviation ratio to the mean, as shown in formula (2), where S_σ is the standard deviation of the GDS S of the specific WL segment, and S_μ is the average value of S.

2. MO(Mode)

The MO is the value with obvious central tendency points in the statistical distribution. In this paper, it is defined as the value most frequently appears in the GDS S.

3. SKW(Coefficient of skewness)

SKW is a measure of the direction and extent of the statistical data's skewness, as indicated by formula (3).

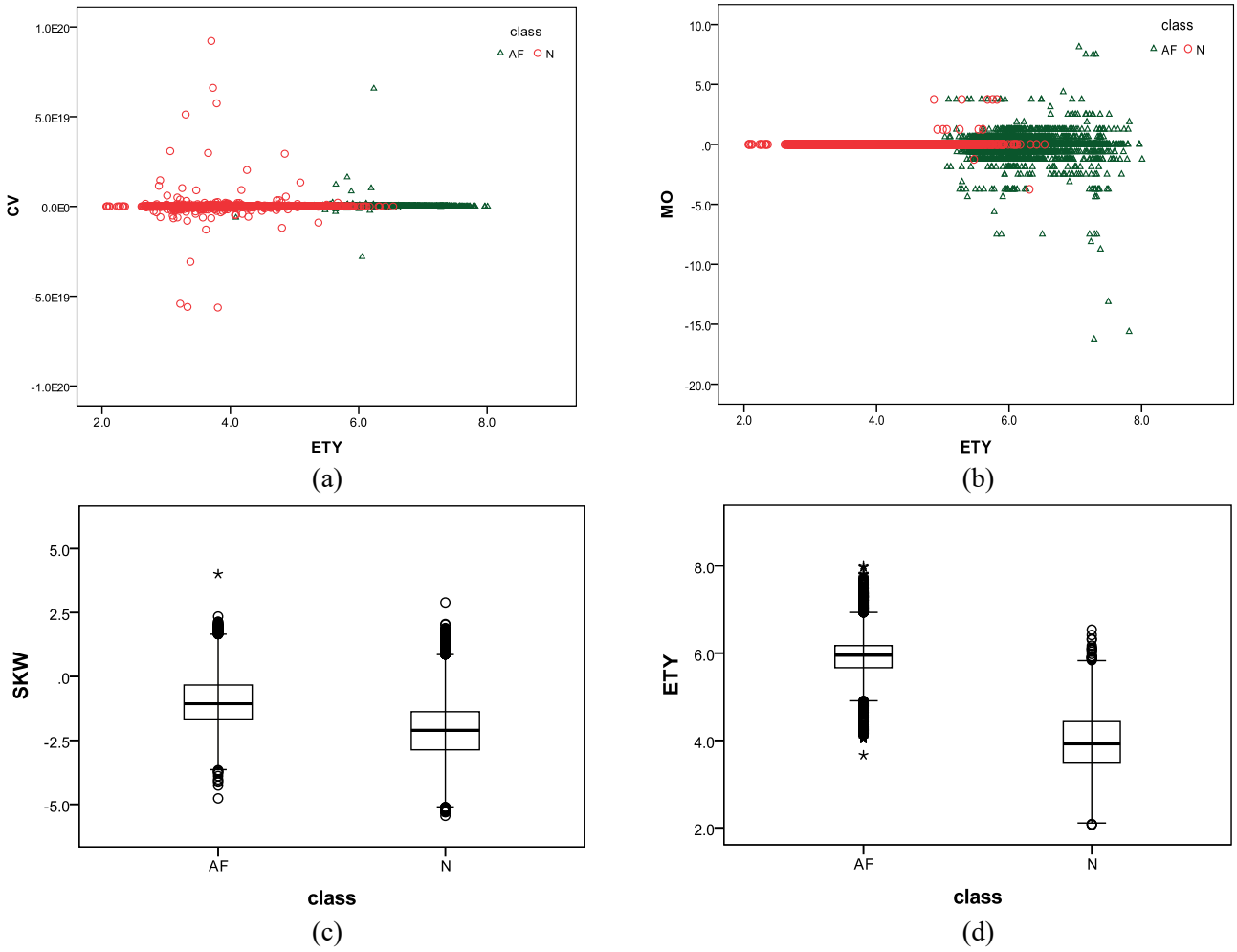

Fig. 4. Comparison of the distribution of feature values between AF class and N class in dataset A. (a) Scatterplot of ETY with CV by class. To improve visualization, feature ETY is used to assist display, because it has the largest difference in distribution between AF class and N class. It is obvious that the distribution of the CV of the AF class is more concentrated. (b) Scatterplot of ETY with MO by class. It is obvious that the distribution of MO of N class is mainly concentrated near 0, while the AF class is widely distributed. (c) Boxplot shows the distribution of SKW, and it is easy to see that the value of class AF is slightly higher than that of N class. (d) Boxplot shows the distribution of ETY, and it is obvious that the value of class AF is higher than that of N class.

$$SKW(S) = E\left[\left((S - S_\mu)/S_\sigma\right)^3\right] \quad (3)$$

4. ETY(Entropy)

ETY clarifies the relationship between probability and information redundancy and provides a quantitative measurement of information.

$$ETY(S) = -\sum_{j=1}^{m} p(S_j)\log_2 p(S_j)(m \le n-1) \quad (4)$$

As shown in formula (4), m distinct values in the GDS S, and $p(S_j)$ represents the probability of taking the j-th value in the gradient set S.

The learning samples composed of the AF specific WL segment's feature set is AF class, and the learning samples composed of the N specific WL segment is N class. Fig. 4 demonstrates an example of comparing the features values distribution of AF class and normal sinus rhythm (N) class. Fig. 4 (a), (b), (c) and (d) are comparisons of CV scatter plot, MO scatter plot, SKW box plot and ETY box plot of AF class and N class, respectively.

Theoretically, it is expected that the CV value of the specific WL AF class is larger than that of the N [4,16]. As shown in Fig. 4 (a), although the CV value of AF class is not significantly larger than the N, it can be easily summarized that the CV value distribution of the AF class is more concentrated. As shown in Fig. 4 (b), the MO of AF class is mostly concentrated in the interval of [−5,5], while the N class value is mostly concentrated on and around 0. It is easy to see from Fig. 4 (c) that the AF class SKW is higher than that of the N class on the whole. Since AF has an irregularly shaped f-wave and the RR interval is not uniform, the AF waveform has greater uncertainty and unpredictability than the normal sinus rhythm waveform. Therefore, theoretically, AF should contain more information than normal sinus rhythm [17]. As shown in Fig. 4 (d), the AF class ETY value is significantly higher than the N class value. That is, the amount of information contained in AF rhythm is indeed greater than normal sinus rhythm.

On the whole, the distribution of each feature is obviously different between AF and N classes. Therefore, we are very optimistic that we can achieve good classification results.

2.4. The detailed process of AF detection based on GDS

The method for detecting AF based on GDS feature extraction proposed in this paper is briefly summarized in Algorithm 1 of Table 1. Here v is the number of raw ECG records; l is the number of samples in the learning sample set obtained after data preprocessing; G(AF/N) represents the set of AF/N segments, so Gt(AF/N) represents the set of AF/N segments of the t-th raw ECG record; g_{tj} represents the j-th AF/N segment of the t-th record; the alternative values for the WL are 2 s, 5 s, 8 s, and 10 s, the optimal WL needs to be determined experimentally; p represents the number of specific WL segments of each AF/N segment; Etq represents the set of specific WL segment of the q-th AF/N segment of the t-th raw ECG record, so e_{tqp} represents the p-th specific WL segment of the q-th AF/N segment of the t-th record.

The calculation of the method proposed in this paper is based on the ECG signal sampling points, and the time is mainly spent on the acquisition of the GDS. The number of sampling points of each WL segment is set to n, then the number of calculations to obtain the GDS of the WL segment is (n-1). And the calculation of the four features traverses the GDS, respectively, so the number of calculations is about 5(n-1), and the time complexity is O(n).

2.5. The proposed DNN (Deep Neural Networks)

A good feature extraction method should be suitable for all types of classifiers, not only for traditional classic classifiers but also for popular deep learning classifiers. So we designed a simple Deep Neural Networks (DNN) to verify the generalization ability of the proposed feature extraction method. As shown in Fig. 5, the DNN is a fully connected neural network, including 3 hidden layers, each hidden layer includes 10 neurons, and the activation function is ReLU.

Table 1
A GDS-based feature extraction method for AF detection.

Algorithm 1 The detailed process of the method for detecting AF based on GDS feature extraction

Input: ECG signal
Output: the predicted labels of testing set:$\hat{y}=(\hat{y}_{(9l/10+1)},\hat{y}_{(9l/10+2)},\ldots\hat{y}_l)$
Procedure
Set $l=0$;
for $t=1,2,\ldots,v$ do
  The AF/N segments intercepting the t-th record constitutes the set G(AF/N):
  Gt(AF/N)={g_{t1}, g_{t2},…, g_{tj}};
  Denoising Gt(AF/N) with Butterworth and Zero Phase Shift Filter
  for $q=1,2,\ldots,j$ do
    p = length(g_{tq})/WL;
    Cutting the AF/N segments into specific WL segments constitutes the set E:
    Etq={e_{tq1}, e_{tq2},…,e_{tqp}};
    for $k=1,2,\ldots p$ do
      Calculate the GDS S_{tqk} of e_{tqk} according to (1);
      $\boldsymbol{x}_{tqk}$ = [$MO(S_{tqk})$, $CV(S_{tqk})$, $SKW(S_{tqk})$, $ETY(S_{tqk})$] according to (2), (3) and (4);
      $\boldsymbol{x}_l \leftarrow \boldsymbol{x}_{tqk}$;
      $\boldsymbol{x}_l$ normalization;
      l++;
    end for
  end for
end for
Get labeled sample set D_l ={($\boldsymbol{x}_1$, y_1), ($\boldsymbol{x}_2$, y_2),…, ($\boldsymbol{x}_l$, y_l)};
$D_l \rightarrow$ varies classifiers(10-fold cross-validation mode)

Calculate the GDS of the specific WL segment and the SKW, CV, MO, and ETY of the GDS as the classifier's input features. And All experiments used the test mode of 10-fold cross-validation.

3. Experiments and results

To verify the effectiveness of the proposed method and determine its optimal processing steps, five comparative experiments were performed: robustness analysis to determine whether denoising is to be performed, normalized analysis to determine whether to perform normalization, and different WL(2/5/8/10 s) segment performance comparison analysis to determine the optimal WL, as well as feature importance analysis, and effectiveness analysis on multiple databases.

3.1. Experimental data

To facilitate our experiments, we used four databases, the MIT-BIH Atrial Fibrillation Database (AFDB) [18,19], the MIT-BIH Normal Sinus Rhythm Database (NSRDB) [18], the MIT-BIH Arrhythmia Database (MITDB) [18,20], and the AF Termination Challenge Database

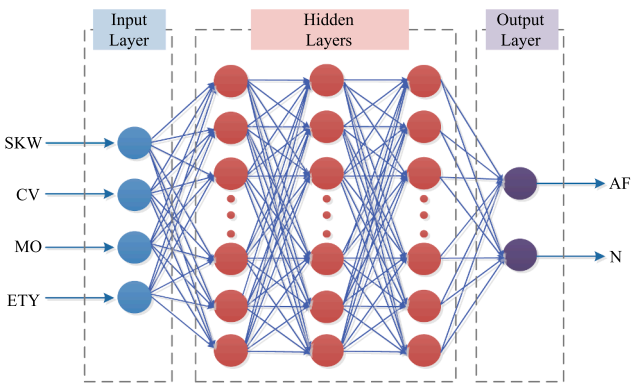

Fig. 5. The structure of DNN.

(AFTDB).[18,21]

The AFDB includes 25 long-term ECG recordings of human subjects with atrial fibrillation (mostly paroxysmal), each of which is about 10 h long, with a sampling frequency of 250 Hz, resolution of 12 bits, and recording bandwidth of 0.1 ~ 40 Hz, and mainly contains rhythm annotations including AF and AFL (atrial flutter). Because the first two records are incomplete, only the remaining 23 records are used.

The NSRDB contains 18 ECG data records with a duration of 24 h and a sampling rate of 128 Hz. No significant arrhythmias were recorded in any of the signals. Data were collected from five males aged 26–45 and 13 females aged 20–50.

The MITDB contains 48 excerpts of two-channel ambulatory ECG recordings, per channel with 11-bit resolution over a 10 mV range, each record with a duration of half an hour and a sampling rate of 360 Hz. It contains heartbeat annotations and rhythm annotations for various arrhythmia diseases. The database is collected from 47 subjects, including 25 men aged 32 to 89 years and 22 women aged 23 to 89 years, among which records 201 and 202 came from the same male subject.

The AFTDB contains 80 one-minute segments of atrial fibrillation, including examples of both sustained and spontaneously terminating AF, collected from 60 different subjects, each record contains two ECG leads, and the sampling rate is 128 per second.

Therefore, based on the description of the 4 databases, it can be roughly counted that the number of subjects in this experiment is 146.

3.2. Experiment design

3.2.1. Data preprocessing

In this paper, five datasets are generated from four databases, as shown in Table 2. The dataset AFNSRs consists of AF rhythm data provided by AFDB and normal sinus rhythm (N) data provided by NSRDB. At the same time, to verify the robustness of the proposed method, two datasets are prepared, the dataset AFNSRs is called dataset A without denoising and is called dataset B after denoising. The AF data and N data of the dataset AFDBs are both from the AFDB database; similarly, the AF data and N data of the dataset MITDBs are both from the MITDB database; in the dataset AFTNSRs, the AF data comes from the database AFTDB, and the N data comes from the database NSRDB; the Combined dataset covers data in datasets AFNSRs, AFDBs, MITDBs, and AFTNSRs.

First, it is necessary to extract the AF/N segments of each ECG record and cut them into specific WL segments. Table 2 takes WL = 10 s as an example, and to maintain the balance of the AF and N data, an approximately equal number of N data are randomly extracted and segmented. For example, the MITDB database extracts a total of 107 AF segments and divides them into 752 10 s segments. At the same time, to maintain dataset balance, 808 10 s segments of N data are randomly extracted.

Then calculate the GDS of each specific WL segment, extract MO, CV, SKW, and ETY of the GDS to form a learning sample, so the number of specific WL segments is also the sample size of the experiment.

The data preprocessing and feature extraction were completed in MATLAB R2014a using the WaveForm DataBase (WFDB) Toolbox for MATLAB [22].

3.2.2. Classification

The Waikato Environment for Knowledge Analysis (WEKA) 3.6 (released in December 2008) [23] was selected as the experimental platform for classification in this paper. WEKA is an open source machine learning and data mining software based on the JAVA environment; it contains data preprocessing, classification analysis, cluster analysis, association rules, attribute selection, data visualization, etc. According to different algorithm principles, WEKA divides all the mainstream classification algorithms into six categories [24]: Bayesian techniques, tree-based classifiers, rule-based classification methods, function-based techniques, lazy methods, and *meta*-techniques. A total of 56 classification algorithms covering six classification models were tested on WEKA.

WEKA is all traditional classification algorithms. To verify whether the GDS-based feature extraction method for AF detection is suitable for popular deep learning algorithms, we tested the performance of our proposed DNN on Python 3.6.

3.2.3. Model evaluation metrics

WEKA has a complete evaluation system, which calculates the confusion matrix and obtains several evaluation metrics. Six metrics were selected in this paper: accuracy, recall, specificity, precision, F-measure, and AUC (area under the ROC curve). F-measure is defined as shown in formula (5). AUC [25] is the area enclosed by the ROC curve and the coordinate axis, and the value ranges between 0.5 and 1. The larger the value, the closer to 1, indicating better classification results.

$$F-\text{measure} = (2 \times Recall \times Precision)/(Recall + Precision) \quad (5)$$

Here, TP (true positive) is the number of AF rhythms correctly detected as AF rhythm; FP (false positive) is the number of normal sinus rhythms wrongly detected as AF rhythm; TN (true negative) is the number of normal sinus rhythms correctly detected as normal sinus rhythm; FN (false negative) is the number of AF rhythms wrongly detected as normal sinus rhythm.

3.3. Experimental results

3.3.1. Analysis of robustness and classifier adaptability

To verify whether the feature extraction method proposed in this paper is sensitive to noise, dataset A (without denoising and WL = 10 s) and dataset B (denoising and WL = 10 s) were classified, respectively. Fifty-seven classification algorithms were involved in the experiment and all used the test mode of 10-fold cross-validation. Due to similar results for each algorithm, a total of 17 representative classification algorithms were selected for all categories to list the results. Table 3 shows

Table 2
Structure description of five datasets.

Dataset	Database									Sum (10 s)		
	AFDB			MITDB			NSRDB	AFTDB				
	AF (seg)	AF (10 s)	N (10 s)	AF (seg)	AF (10 s)	N (10 s)	N (10 s)	AF (seg)	AF (10 s)	Sum (AF)	Sum (N)	Sum (all)
AFNSRs(A/B)	258	9391					9000			9391	9000	18,391
AFDBs	258	9391	9000							9391	9000	18,391
MITDBs				107	752	808				752	808	1560
AFTNSRs							500	80	480	480	500	980
Combined	258	9391	4300	107	752	808	5500		480	10,623	10,608	21,231

Annotation: AF (seg): number of complete AF rhythm segments cut from ECG records; AF (10 s): number of WL = 10 s segments cut from the AF rhythm segment; N (10 s): number of WL = 10 s segments cut from the normal sinus rhythm segment; Sum (AF): total number of 10 s AF rhythm segments; Sum (N): total number of 10 s normal sinus rhythm segments; sum (all): total number of 10 s AF rhythm and normal sinus rhythm segments.

Table 3
Classification results for dataset A (without denoising).

Algorithm	Accuracy	Recall	Specificity	Precision	F-Measure	AUC
BayesNet [26]	97%	97.7%	96.3%	96.5%	97.1%	0.992
MLP [27]	98.3%	99%	97.6%	97.8%	98.4%	0.995
IB1 [28]	97.8%	97.9%	97.8%	97.9%	97.9%	0.978
KStar [29]	96%	98.7%	93.3%	93.9%	96.2%	0.995
Bagging [30]	98.4%	98.9%	97.9%	98%	98.4%	0.997
Decorate [31]	98.3%	99%	97.7%	97.8%	98.4%	0.995
Ensemble Selection [32]	98.3%	98.9%	97.7%	97.8%	98.4%	0.996
Random Committee [33]	98.3%	98.7%	97.8%	97.9%	98.3%	0.992
Rotation Forest [34]	98.5%	99.2%	97.8%	97.9%	98.5%	0.996
DTNB [35]	97.9%	98.8%	97%	97.2%	98%	0.996
JRip [36]	98.3%	99%	97.5%	97.6%	98.3%	0.987
PART [37]	98.2%	98.8%	97.6%	97.7%	98.3%	0.995
J48 [38]	98.3%	99.2%	97.5%	97.6%	98.4%	0.991
LMT [39]	98.4%	99%	97.8%	97.9%	98.4%	0.997
Random Forest [40]	98.3%	98.9%	97.7%	97.8%	98.4%	0.994
REPTree [41]	98.4%	98.8%	97.8%	97.9%	98.4%	0.992
DNN	99.2%	98.5%	100%	100%	99.2%	0.993

the results for dataset A, and Table 4 shows the results for dataset B.

It is obvious that all the classifiers have achieved high performance, and the performance of our proposed DNN is the best. It can be seen from Table 3 and Table 4 that the results for each algorithm in the two datasets are very similar, and the AUC values of most algorithms are up to 0.99. On the whole, the results for dataset A are slightly higher than for dataset B. The reason may be that some subtle information of the signal is filtered out during the filtering process, but there are some algorithms whose evaluation metric dataset B is higher than or equal to dataset A, as shown in bold in Table 4. Therefore, it can be concluded that the method is insensitive to noise.

On the other hand, the results we obtained on the 57 algorithms covering all categories classification models are similar to those listed, whether denoising or not. It can be concluded that the feature extraction method proposed in this paper is suitable for most classifiers.

3.3.2. *Normalization analysis*

The range of values of each feature varies greatly. Therefore, the zero-mean normalization function of IBM SPSS Statistics 20.0 [42] was used to normalize all features. After normalization, some algorithms are improved in performance, while others are reduced. Table 5 and Fig. 6. show the results of comparative experiments performed on datasets MITDBs and AFNSRs without denoising and WL = 10 s. It is not difficult to determine that the normalization effect is very unstable. Therefore, the method proposed in this paper can be used without normalization.

3.3.3. *Performance comparison of different window lengths(WL)*

To find the optimal WL, dataset A is cut into datasets with WL of 2 s, 5 s, 8 s, and 10 s, respectively. Since paroxysmal AF sometimes has a very short duration and the duration of a static ECG is generally less than 10 s, the maximum value was set to 10 s. The experimental results are shown in Table 6 and Fig. 7., with an increase of the WL, the AF detection effect gets better and better, and the optimal WL is 10 s. This result can be explained by the fact that the larger the data volume, the more obvious the data distribution characteristics. But it is worth noting that it has good performance even when WL = 2 s, indicating that this method is also suitable for AF detection in short-term ECG segments.

3.3.4. *Analysis of the importance and necessity of features*

To analyze the importance and necessity of statistical distribution features CV, MO, SKW, and information feature ETY for AF detection, four experiments were designed, one feature was removed each time for AF detection. Comparison of the four test results allows analysis of the features' importance, the four results are compared with those in Table 3 (the original result, that is, all features included in the test) to analyze the necessity of the features. Here, the Random Committee [33] algorithm is taken as an example, and the experiment was performed on dataset A (WL = 10 s).

The detection results are shown in Table 7 of the features CV, MO, SKW, and ETY were removed in order, and the last row of the table is the original result. It is easy to see that the result of removing ETY is the most unsatisfactory, and the accuracy of 69.2% is far lower than the accuracy of 98.3% of the original result. Therefore, the feature ETY is the

Table 4
Classification results for dataset B (with denoising).

Algorithm	Accuracy	Recall	Specificity	Precision	F-Measure	AUC
BayesNet [26]	93.6%	**98.2%**	88.9%	90.2%	94%	0.988
MLP [27]	96.7%	96.8%	96.5%	96.7%	96.8%	0.993
IB1 [28]	96.5%	96.5%	96.5%	96.6%	96.6%	0.965
KStar [29]	95.8%	95.8%	**95.7%**	**95.9%**	95.9%	0.984
Bagging [30]	97.5%	97.9%	97%	97.2%	97.5%	0.996
Decorate [31]	97.2%	97.5%	96.8%	97%	97.2%	0.993
Ensemble Selection [32]	97.4%	97.9%	96.9%	97.1%	97.5%	**0.996**
Random Committee [33]	97.4%	97.8%	97%	97.1%	97.5%	0.991
Rotation Forest [34]	97.5%	97.9%	97.1%	97.2%	97.5%	0.996
DTNB [35]	96.3%	96.6%	96.1%	96.3%	96.4%	0.994
JRip [36]	97.1%	97.5%	96.7%	96.8%	97.2%	0.981
PART [37]	96.9%	96.3%	**97.6%**	97.6%	97%	0.994
J48 [38]	97.3%	97.8%	96.9%	97%	97.4%	0.989
LMT [39]	97.2%	97.3%	97.1%	97.3%	97.3%	0.994
Random Forest [40]	97.5%	98.1%	96.9%	97.1%	97.6%	0.993
REPTree [41]	97.2%	97.8%	96.7%	96.8%	97.3%	0.99
DNN	98.5%	97.1%	100%	100%	98.5%	0.986

Table 5
Performance comparison of normalized and non-normalized.

Algorithm	MITDBs				AFNSRs			
	Unnormalized		Normalized		Unnormalized		Normalized	
	Accuracy	Recall	Accuracy	Recall	Accuracy	Recall	Accuracy	Recall
BayesNet [26]	93.5%	94%	93.5%	94%	97%	97.7%	97.1%	98%
MLP [27]	93.3%	92%	93.3%	92%	98.32%	99%	98.34%	99.1%
Bagging [30]	94.6%	93.6%	94.6%	93.9%	98.40%	98.9%	98.42%	98.9%
PART [37]	94.5%	94.4%	94.2%	94.4%	98.21%	98.8%	98.18%	99%
J48 [38]	94.9%	93.8%	94.6%	93.9%	98.35%	99.2%	98.37%	99.2%
Random Forest [40]	94.4%	93.8%	94.2%	94.4%	98.33%	98.9%	98.28%	98.8%
DNN	97.4%	94.7%	97.42%	94.67%	99.2%	98.5%	99.18%	98.40%

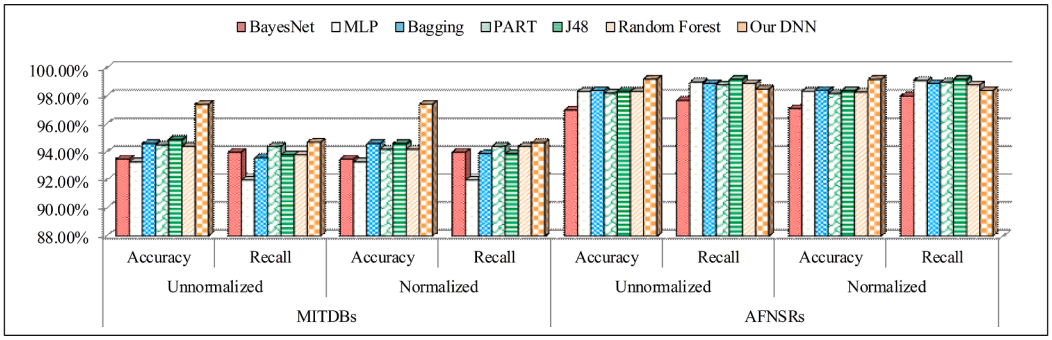

Fig. 6. Performance comparison histogram of normalization and non-normalization.

Table 6
Performance comparison analysis of different WL (2/5/8/10 s).

Algorithm	2 s		5 s		8 s		10 s	
	Accuracy	Recall	Accuracy	Recall	Accuracy	Recall	Accuracy	Recall
BayesNet [26]	92.2%	93.4%	92.6%	95.6%	95.2%	98.3%	97%	97.7%
MLP [27]	92%	94%	93.3%	95.6%	95%	97.5%	98.3%	99%
IB1 [28]	90.8%	90.5%	92%	92%	94.3%	94.3%	97.8%	97.9%
Rotation Forest [34]	93.5%	95.7%	94.3%	96.7%	96.2%	98.3%	98.5%	99.2%
DTNB [35]	93.3%	95.2%	94.1%	96.1%	96%	98.2%	97.9%	98.8%
REPTree [41]	93.4%	95%	94.2%	96.1%	96.1%	97.8%	98.4%	98.8%
DNN	92.06%	90.96%	93.39%	94.78%	97.93%	98.51%	99.2%	98.5%

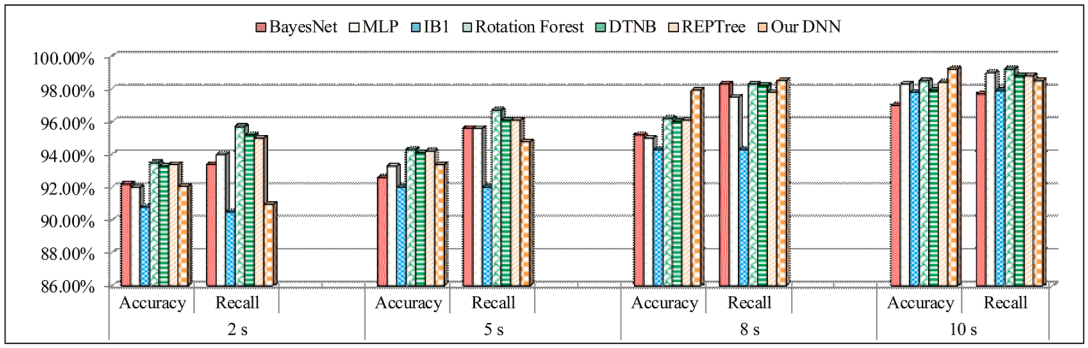

Fig. 7. Performance comparison histograms for different WLs.

most important, followed by SKW, CV, and MO. At the same time, it is easy to find that no matter which feature is removed, none of the evaluation metrics are higher than the original result, so the four features are all essential for AF detect.

ETY describes the amount of information carried by the signal and the complexity of the signal. The result shows that ETY is the most significant for performance. On the other hand, the information quantity and complexity of the AF class and N class signals are quite different. Combined with the other three features, this not only proves that ETY can extract AF signal's characteristics well, that is, f-wave with different shapes and irregular RR intervals. It also proves that the GDS-based features extracted in this paper are effective.

3.3.5. AF detection results for different datasets

Table 2 details the structure of five datasets consisting of four databases AFDB, NSRDB, MITDB, and AFTDB. Table 8 shows the five

Table 7
Analysis of the importance and necessity of features.

Remove	Accuracy	Recall	Specificity	Precision	F-Measure	AUC
CV	97.8%	97.8%	97.7%	97.8%	97.8%	0.978
MO	97.8%	97.8%	97.8%	97.8%	97.8%	0.978
SKW	94.8%	95%	94.7%	94.9%	94.9%	0.948
ETY	69.2%	69.7%	68.8%	70%	69.8%	0.692
NONE	98.3%	98.7%	97.8%	97.9%	98.3%	0.992

datasets' performance (without denoising, unnormalized, and WL = 10 s) on five classical classification algorithms. It is not difficult to see that the performance for AFNSRs and AFTNSRs are the best, followed by that are AFDBs, MITDBs, and Combined, the overall detection performance is close to 97%, which proves that the GDS-based feature extraction method for AF detection proposed in this paper is effective. It is worth mentioning that our proposed CNN has achieved the best performance.

4. Discussion

Through the above five experimental analysis, the following conclusions can be obtained: 1) in the data preprocessing step, no denoising and normalization are needed, which shows that the GDS-based feature extraction method has good robustness; 2) in the classification step, experiments prove that the method is suitable for most classifiers, indicating that the method has good generalization ability and its features are not limited by the classifier categories; 3) the information quantity feature ETY has the greatest effect on classification performance, and all features have an impact on performance, indicating that the feature set(*SKW*, *CV*, *MO* and *ETY*) extracted based on GDS in this paper is very representative; 4) the method is also suitable for the detection of AF in short-term ECG, and the longer the WL is, the better the performance is; 5)it has achieved good results on different databases, so in summary, the GDS-based feature extraction method proposed in this paper is effective.

At present, many researchers are working on the automatic detection of AF, as shown in Table 9, which lists the comparative analysis of representative methods since 2008 on the database AFDB (same as dataset AFDBs). Most of the methods, including methods 1[43], 2 [44], 3 [17], 4 [45], and 5 [5] are based on RRI; such methods first need beat detection, and the WL is between 31 ~ 128 beats, indicating that there are limitations in short-term ECG detection. Although method 2 [44] does not explicitly explain WL, the summary clearly states that its limitation is that it cannot detect short-term (such as 10 s) ECG. The main difficulty of the PWA-based method is the detection of the P wave. Because the P wave is extremely easy to miss, this method requires higher signal quality, the methods 6 [11] and 7 [46] explicitly propose to denoise or need to be combined with other features, such as methods 7 [46] and 8 [47]. Methods 9 [13]and 10[48] are based on SWT and AR coefficients, respectively. Although such methods do not require beat detection, they require high signal quality and require denoising processing.

In disease diagnosis, the most important thing is to reduce the missed diagnosis rate and misdiagnosis rate. Therefore, recall and specificity are the most commonly used evaluation indicators. The Recall is also called True Positive Rate (TPR), where it represents the proportion of AF patients who are correctly diagnosed as AF. The Specificity is also called True Negative Rate (TNR), which means the proportion of healthy people who are correctly diagnosed as healthy. In many AF automatic diagnosis studies, only performance recall and specificity are described. As shown in Table 9, the GDS-based method proposed in this paper does not require beat detection and does not require denoising. By comparing WL, it is found that most of the WLs are larger than the WL (10 s) of our proposed method, while the WLs of methods 6[11], 7[46], 8[47], and 10 [48] are closer to 10 s, but the performance of Recall and Specificity were lower than that of the proposed method. And the method we proposed gets the highest performance with an accuracy of 99%, a recall of 99.7%, and a specificity of 98.2%. Therefore, the feature extraction method based on GDS proposed in this paper is a good choice in the detection of AF.

5. Conclusion and further research

Current research indicates that the feature extraction method based

Table 8
Atrial fibrillation detection results using feature extraction method based on GDS.

Dataset	Bagging [30](%)			En-Selection [32] (%)			PART [37] (%)			J48 [38] (%)			DNN(%)		
	Acc	Rec	Spe	Acc	Rec	Spe	Acc	Rec	Spe	Acc	Rec	Spe	Acc	Rec	Spe
AFNSRs	98.4	98.9	97.9	98.3	98.9	97.7	98.2	98.8	97.6	98.4	99.2	97.5	99.2	98.5	100
AFDBs	95.9	94.2	97.8	95.9	93.9	98	95.6	93.7	97.6	95.8	93.9	97.8	99	99.7	98.2
MITDBs	94.6	93.6	95.4	94.1	92.7	95.4	94.5	94.4	94.6	94.9	93.8	96	97.4	94.7	100
AFTNSRs	99.3	99.6	99	98.8	98.8	98.8	99.5	99.8	99.2	99.4	99.6	99.2	100	100	100
Combined	94.3	93.7	94.9	94.2	93.6	94.9	93.8	92.7	94.9	94.2	93.6	94.8	98.3	96.7	100

Annotation: En-Selection:Ensemble Selection; Acc: Accuracy; Rec: Recall; Spe: Specificity.

Table 9
Comparison of the performance of recent AF detection algorithms on AFDB.

ID	Method	Features	Beat detection	Denoising	WL	Accuracy	Recall	Specificity
1	Lian et al. [43]	RRI	Yes	—	128 beats	—	95.8%	96.4%
2	Zhou et al. [44]	RRI	Yes	Yes	—	97.50%	96.82%	98.06%
3	Li [17]	RRI	Yes	—	40 s	95.9%	95.3%	96.3%
4	Afdala et al. [45]	RRI	Yes	Yes	40 s	89.79%	91.04%	89.01%
5	Andersen et al. [5]	RRI	Yes	—	31 beats	97.80%	98.98%	96.95%
6	Ladavich [11]	PWA	Yes	Yes	1 beat	—	89.37%	89.54%
					7 beats	—	98.09%	91.66%
7	Couceiro et al. [46]	PWA + RRI + AA	Yes	Yes	>12 beats	—	93.8%	96.09%
8	Rincón et al. [47]	PWA + HBR (RRI)	Yes	—	10 s	—	96%	93%
9	Shadnaz Asgari et al. [13]	SWT	No	Yes	30 s	97.1%	97.0%	97.1%
10	Parvaresh et al. [48]	AR coefficients	No	Yes	15 s	—	96.14%	93.20%
11	This paper(GDS + DNN)	GDS	No	No	10 s	99%	99.7%	98.2%

Annotation: PWA: P-wave absence; RRI: RR intervals; AA: atrial activity; AR coefficients: autoregressive coefficients; HBR: heartbeat rate; HBR (RRI): heartbeat rate analysis is based on R–R interval variance; SWT: stationary wavelet transform; GDS: gradient set; '—' indicates not mentioned in the paper.

on GDS proposed for detecting AF does not require noise reduction, does not require beat detection or complex mathematical transformation, and nor does it need normalization of the feature set to be input to the classifier. It shows good performance on 5 datasets composed of 4 databases not only suitable for the vast majority of classifiers but also AF detection in short-term ECG. At the same time, the method achieves the best performance on our proposed DNN classifier. Therefore, this method is a good choice for feature extraction in AF detection. In the future, the feature extraction method needs to be further improved, such as improving AF detection performance by proposing a more representative feature set or combining it with other types of features, and can also be extended to other directions of ECG intelligent assisted detection.

Funding

This work is supported by The Key Research, Development, and Dissemination Program of Henan Province (Science and Technology for the People)(No. 182207310002).

CRediT authorship contribution statement

Haiyan Wang: Conceptualization, Methodology, Software, Validation, Writing - original draft. **Honghua Dai:** Validation, Formal analysis, Writing - review & editing. **Yanjie Zhou:** Visualization, Resources, Writing - review & editing. **Bing Zhou:** Software, Investigation, Supervision. **Peng Lu:** Software, Investigation. **Hongpo Zhang:** Data curation, Investigation. **Zongmin Wang:** Conceptualization, Project administration, Funding acquisition.

Declaration of Competing Interest

The authors declare that they have no known competing financial interests or personal relationships that could have appeared to influence the work reported in this paper.

References

[1] S. Petrutiu, J. Ng, G.M. Nijm, H. Al-Angari, S. Swiryn, A.V. Sahakian, Atrial fibrillation and waveform characterization, IEEE Eng. Med. Biol. Mag. 25 (2006) 24–30.
[2] J. Lee, B.A. Reyes, D.D. McManus, O. Maitas, K.H. Chon, Atrial fibrillation detection using an iPhone 4S, IEEE Trans. Biomed. Eng. 60 (1) (2013) 203–206.
[3] N. Sadr, M. Jayawardhana, T.T. Pham, R. Tang, A.T. Balaei, P. de Chazal, A low-complexity algorithm for detection of atrial fibrillation using an ECG, Physiol. Meas. 39 (6) (2018) 064003, https://doi.org/10.1088/1361-6579/aac76c.
[4] A. Kennedy, D.D. Finlay, D. Guldenring, R.R. Bond, K. Moran, J. McLaughlin, Automated detection of atrial fibrillation using RR intervals and multivariate-based classification, J. Electrocardiol. 49 (6) (2016) 871–876.
[5] R.S. Andersen, A. Peimankar, S. Puthusserypady, A deep learning approach for real-time detection of atrial fibrillation, Expert Syst. Appl. 115 (2019) 465–473.
[6] X. Zhou, H. Ding, W. Wu, Y. Zhang, A real-time atrial fibrillation detection algorithm based on the instantaneous state of heart rate, PLoS One, 10 (2015) e0136544.
[7] O. Andersson, K.H. Chon, L. Sornmo, J.N. Rodrigues, A 290mv sub-vt asic for real-time atrial fibrillation detection, IEEE Trans. Biomed. Circuits Syst. 9 (2014) 377–386.
[8] N. Larburu, T. Lopetegi, I. Romero, Comparative study of algorithms for atrial fibrillation detection, in:2011 Computing in Cardiology, IEEE (2011) 265–268.
[9] I. Christov, G. Bortolan, I. Daskalov, Sequential analysis for automatic detection of atrial fibrillation and flutter, in, Computers in Cardiology, IEEE (2001) 293–296.
[10] J. Carlson, R. Johansson, S.B. Olsson, Classification of electrocardiographic P-wave morphology, IEEE Trans. Biomed. Eng. 48 (4) (2001) 401–405.
[11] S. Ladavich, B. Ghoraani, Rate-independent detection of atrial fibrillation by statistical modeling of atrial activity, Biomed. Signal Process. Control. 18 (2015) 274–281.
[12] N. Liu, M. Sun, L. Wang, W. Zhou, H. Dang, X. Zhou, A support vector machine approach for AF classification from a short single-lead ECG recording, Physiol. Meas. 39 (2018), 064004.
[13] S. Asgari, A. Mehrnia, M. Moussavi, Automatic detection of atrial fibrillation using stationary wavelet transform and support vector machine, Comput. Biol. Med. 60 (2015) 132–142.
[14] Yong Xia, Naren Wulan, Kuanquan Wang, Henggui Zhang, Detecting atrial fibrillation by deep convolutional neural networks, Computers in Biology and Medicine 93 (2018) 84–92.
[15] B. Pourbabaee, M.J. Roshtkhari, K. Khorasani, Deep convolutional neural networks and learning ECG features for screening paroxysmal atrial fibrillation patients, IEEE Trans. Syst. Man Cybern. Syst. 48 (12) (2018) 2095–2104.
[16] K. Tateno, L. Glass, Automatic detection of atrial fibrillation using the coefficient of variation and density histograms of RR and ΔRR intervals, Med. Biol. Eng. Comput. 39 (6) (2001) 664–671.
[17] Y. Li, X. Tang, A. Wang, H. Tang, Probability density distribution of delta RR intervals: a novel method for the detection of atrial fibrillation, Australas. Phys. Eng. Sci. Med. 40 (3) (2017) 707–716.
[18] A.L. Goldberger, L.A.N. Amaral, L. Glass, J.M. Hausdorff, P.C. Ivanov, R.G. Mark, J. E. Mietus, G.B. Moody, C.-K. Peng, H.E. Stanley, PhysioBank, PhysioToolkit, and PhysioNet: components of a new research resource for complex physiologic signals, Circulation 101 (2000) e215–e220.
[19] G. Moody, A new method for detecting atrial fibrillation using RR intervals, Comput. Cardiol. 227–230 (1983).
[20] G.B. Moody, R.G. Mark, The impact of the MIT-BIH arrhythmia database, IEEE Eng. Med. Biol. Mag. 20 (3) (2001) 45–50.
[21] G.B. Moody, Spontaneous termination of atrial fibrillation: A challenge from PhysioNet and computers in cardiology 2004, in: In: Computers in Cardiology, 2004, pp. 101–104.
[22] I. Silva, G.B. Moody, An open-source toolbox for analysing and processing physionet databases in matlab and octave, J. Open. Res. Softw. 2 (2014) 1–7.
[23] M. Hall, E. Frank, G. Holmes, B. Pfahringer, P. Reutemann, I.H. Witten, The WEKA data mining software: an update, ACM SIGKDD explorations newsletter 11 (1) (2009) 10–18.
[24] E. Frank, M. Hall, G. Holmes, R. Kirkby, B. Pfahringer, I.H. Witten, L. Trigg, in: Data Mining and Knowledge Discovery Handbook, Springer US, Boston, MA, 2010, pp. 1269–1277, https://doi.org/10.1007/978-0-387-09823-4_66.
[25] J. Han, M. Kamber, Data mining: concepts and techniques, Second Edition (2006).
[26] S.M. Weiss, C.A. Kulikowski, Computer systems that learn: classification and prediction methods from statistics, neural nets, machine learning, and expert systems, Morgan Kaufmann Publishers Inc., (1991).
[27] D.E. Rumelhart, G.E. Hinton, R.J. Williams, Learning representations by back-propagating errors, Nature 323 (1986) 533–536.
[28] T. Cover, P. Hart, Nearest neighbor pattern classification, IEEE Trans. Inf. Theory. 13 (1) (1967) 21–27.
[29] J.G. Cleary, L.E. Trigg, et al., K*: An instance-based learner using an entropic distance measure, in: Proceedings of the 12th International Conference on Machine Learning, Vol. 5, 1995, pp. 108–114..
[30] L. Breiman, Bagging predictors, Machine learning 24 (1996) 123–140.
[31] P. Melville, R.J. Mooney, Constructing diverse classifier ensembles using artificial training examples, in: Proceedings of the 18th international joint conference on Artificial intelligence (IJCAI), 2003, pp. 505-510.
[32] R. Caruana, A. Niculescu-Mizil, G. Crew, A. Ksikes, Ensemble selection from libraries of models, in: Proceedings of the International Conference on Machine Learning (ICML), ACM, 2004, pp. 1-9.
[33] I.H. Witten, E. Frank, M.A. Hall, Data mining: practical machine learning tools and techniques, Elsevier, 2011.
[34] J.J. Rodriguez, L.I. Kuncheva, C.J. Alonso, Rotation forest: A new classifier ensemble method, IEEE Trans. Pattern Anal. Mach. Intell. 28 (10) (2006) 1619–1630.
[35] M.A. Hall, E. Frank, Combining naive bayes and decision tables , in: Proceedings of the 21st Florida Artificial Intelligence Society Conference (FLAIRS), 2008, pp. 318-319.
[36] W.W. Cohen, Fast effective rule induction, in: Proceedings of the Twelfth International Conference on Machine Learning, Elsevier, (1995):115-123.
[37] E. Frank, I.H. Witten, Generating accurate rule sets without global optimization. in: The Fifteenth International Conference on Machine Learning, 1998, pp. 144–151.
[38] J.R. Quinlan, C 4.5: Programs for machine learning, The Morgan Kaufmann Series in Machine Learning, San Mateo, CA: Morgan Kaufmann, (1993).
[39] N. Landwehr, M. Hall, E. Frank, Logistic model trees, Machine learning 59 (2005) 161–205.
[40] L. Breiman, Random forests, Machine learning 45 (2001) 5–32.
[41] J.R. Quinlan, Simplifying decision trees, Int. J. Man Mach. Stud. 27 (3) (1987) 221–234.
[42] I. Spss, IBM SPSS statistics for windows, version 20.0, IBM Corp, New York, 2011, p. 440.
[43] Jie Lian, Lian Wang, Dirk Muessig, A simple method to detect atrial fibrillation using RR intervals, Am. J. Cardiol. 107 (10) (2011) 1494–1497.
[44] Xiaolin Zhou, Hongxia Ding, Benjamin Ung, Emma Pickwell-MacPherson, Yuanting Zhang, Automatic online detection of atrial fibrillation based on symbolic dynamics and shannon entropy, Biomed. Eng. Online. 13 (1) (2014) 18, https://doi.org/10.1186/1475-925X-13-18.
[45] A. Afdala, N. Nuryani, A.S. Nugroho, Automatic detection of atrial fibrillation using basic shannon entropy of RR interval feature, in: Journal of Physics: Conference Series, IOP Publishing, 2017, pp. 1-5.
[46] R. Couceiro, P. Carvalho, J. Henriques, M. Antunes, M. Harris, J. Habetha, Detection of atrial fibrillation using model-based ECG analysis, in: IEEE 2008 19th International Conference on Pattern Recognition, IEEE, 2008, pp.1-5.
[47] F. Rincón, P.R. Grassi, N. Khaled, D. Atienza, D. Sciuto, Automated real-time atrial fibrillation detection on a wearable wireless sensor platform, in: Proceedings of 34th IEEE Annual International Conference of the Engineering in Medicine and Biology Society (EMBC), IEEE, 2012, pp. 2472-2475.
[48] S. Parvaresh, A. Ayatollahi, Automatic atrial fibrillation detection using autoregressive modeling, in: International Conference on Biomedical Engineering and Technology, IPCBEE, 2011, pp,105-108.